Fluid Phase Equilibria 555 (2022) 113346

Contents lists available at ScienceDirect

Fluid Phase Equilibria

journal homepage: www.elsevier.com/locate/fluid

Dielectric constant of mixed solvents based on perturbation theory

Lisa Neumaier[a], Johannes Schilling[a], André Bardow[a,b,*], Joachim Gross[c,*]

[a] Energy & Process Systems Engineering, Department of Mechanical and Process Engineering, ETH Zurich, Tannenstrasse 3, Zurich 8092, Switzerland
[b] Institute of Energy and Climate Research - Energy Systems Engineering (IEK-10), Forschungszentrum Jülich GmbH, Wilhelm-Johnen-Strasse, Jülich 52425, Germany
[c] Institute of Thermodynamics and Thermal Process Engineering, University of Stuttgart, Pfaffenwaldring 9, Stuttgart 70569, Germany

ARTICLE INFO

Article history:
Received 30 September 2021
Revised 22 November 2021
Accepted 26 November 2021
Available online 30 November 2021

Keywords:
Relative static permittivity
Electrolyte equation of state
Ion solution
Electrolyte thermodynamics
Predictive thermodynamics

ABSTRACT

Industrial applications such as batteries and bio-separations require modeling the thermodynamic properties of mixed solvent electrolytes. Thermodynamic models for electrolytes often consider the solvents as a dielectric continuum characterized by their dielectric constant. Therefore, accurate predictions require a physically sound model for the dielectric constant of mixed solvents, depending on temperature, pressure, and mixture composition. We present a physical model for the dielectric constant of pure solvents and mixtures based on perturbation theory. The analytical expression is third order in the dipole density. For each pure component, the model requires the dipole moment and two adjustable pure-component parameters. We apply the model to the binary mixtures methanol–water and ethylene glycol–water considering pure component experimental data for temperatures between 273.15 K to 823.15 K and pressures between 0.1 MPa and 1189.0 MPa. The presented model improves the prediction of the mixed solvent dielectric constant for both mixtures compared to the linear molar mixing rule, and achieves similar accuracies as the linear volume-based and mass-based mixing rules. We show that the model is suitable in the case of scarce experimental data.

1. Introduction

Mixed solvents are promising for electrochemical processes, e.g., batteries [1], co-electrolysis of CO_2 [2], and chemical processes with electrolyte systems, e.g., amine-based CO_2-capture [3]. Modeling these processes requires a thermodynamic model for the electrolyte system. For the design of the process, the used thermodynamic models should predict thermodynamic properties also for electrolyte systems and operating settings where no or few experimental data are available.

For this purpose, electrolyte equations of state (e-EoS) are promising tools. In e-EoS, two approaches are distinguished for modeling the ion-solvent solution: non-primitive and primitive models [4,5]. In non-primitive models, the solvent is described explicitly, as dipolar or multipolar molecules with defined intermolecular (pair) potentials [5–7]. In contrast, primitive models treat the solvent implicitly, as a dielectric continuum [4,5]. Currently, the primitive approach is more established for engineering applications while the non-primitive approach is still at an early stage of development [4–8].

The primitive approach characterizes the solvent as a dielectric continuum with its dielectric constant ε_r, depending on temperature and density [9]. For mixed solvents, the dielectric constant ε_r additionally depends on the mixture composition. Thus, the primitive approach requires a physically sound model for the dielectric constant ε_r of the mixed solvent as one input for an accurate prediction of thermodynamic properties. In particular, the dielectric constant ε_r has to be defined as a function of temperature, pressure, composition (T, p, $\mathbf{x}$) or temperature, density, composition (T, ρ, $\mathbf{x}$) with sufficient accuracy, because the derivatives of the dielectric constant ε_r with respect to these quantities enter the calculation of, e.g., enthalpy and chemical potentials of the electrolyte solution. The impact of ions on the dielectric constant, particularly at high ion concentrations, is not considered in this work.

In the literature, the dielectric constant of the mixed solvent ε_r is frequently modeled with simple mixing rules that mix either the pure component dielectric constants $\varepsilon_{r,i}$ or the pure component polarizations p_i. The most common approach within existing e-EoS is to mix the pure component dielectric constants $\varepsilon_{r,i}$ of all n components linearly based on the mole, volume, or mass fraction

* Corresponding authors.
E-mail addresses: abardow@ethz.ch (A. Bardow), gross@itt.uni-stuttgart.de (J. Gross).

https://doi.org/10.1016/j.fluid.2021.113346

Φ_i of component i [10–13] according to

$$\varepsilon_r = \sum_{i=1}^{n} \Phi_i \varepsilon_{r,i}. \tag{1}$$

Here, the pure component dielectric constants $\varepsilon_{r,i}(T, p)$ are usually taken from empirical correlations, from experimental data, or from molecular simulations [14,15] at temperature T and pressure p of the mixture. Additionally, the ionic influence on the dielectric constant ε_r can be considered by introducing a concentration dependence [16] or by empirically correcting the mixed solvent dielectric constant [17].

Alternatively, the dielectric constant ε_r can be calculated from the polarization p by

$$p = \frac{(\varepsilon_r - 1)(2\varepsilon_r + 1)}{9\varepsilon_r}. \tag{2}$$

The mixed solvent polarization p can be obtained by mixing the pure component polarizations p_i which can be calculated based on Kirkwood [18] from

$$v_i \cdot p_i = \frac{4\pi N_A}{3}\left(\alpha_i + \frac{\mu_i^2 g_i}{3k_B T}\right) \tag{3}$$

with the Avogadro constant N_A, the pure component molar volume v_i, the polarizability α_i, the dipole moment μ_i, the Boltzmann constant k_B, the temperature T, and the g-factor g_i. The g-factor g_i is a measure for the correlation between neighbouring dipoles [19] and must be computed or determined from experimental data.

A prominent mixing approach for polarizations p is Oster's rule [19]. Oster's rule calculates the mixture's polarization p by mixing the pure component polarization p_i based on the mole fraction x_i and the molar volume v_i of pure component i [19]:

$$p = \rho \sum_{i=1}^{n} x_i v_i p_i, \tag{4}$$

where ρ is the molar mixture density. To avoid evaluating mixture densities, the simplified Oster's rule has been developed, which mixes the pure component polarizations p_i based on the volume fraction $\Phi_{v,i}$ calculated from the volumes prior to mixing [19]:

$$p = \sum_{i=1}^{n} \Phi_{v,i} p_i \tag{5}$$

Simple mixing rules, such as Equations (1), (4), or (5) have conceptual deficiencies. These deficiencies become obvious when considering a solvent with a dissolved gas, e.g., carbon monoxide, at $T = 300\,\mathrm{K}$. The pure component dielectric constant $\varepsilon_{r,i}$ of carbon monoxide will be that of a pure gaseous phase, which does not yield a sound contribution to a liquid phase dielectric constant through a mixing rule (Equations (1), (4), or (5), or alike). This problem appears even for a binary mixture of, e.g., water and methanol at bubble point conditions. Additionally, most simple mixing rules neglect the non-ideality of mixtures and thus lack accuracy.

The accuracy can be improved by refining the simple mixing rules with binary parameters from experimental data [19,20] or by using empirical correlations or mixing rules. For empirical correlations, parameters a_i are fitted to mixture data. For example, Amirjahed and Blake [21] calculate the dielectric constant ε_r of a binary mixture as a polynomial depending on the mole fraction of one component x_1 according to

$$\varepsilon_r = a_0 + a_1 x_1 + a_2 x_1^2 + \ldots, \tag{6}$$

and Jouyban et al. [22] according to

$$\ln \varepsilon_r = \frac{a_0 + a_1 x_1}{a_2 + a_3 x_1}. \tag{7}$$

To capture the (T, p, $\mathbf{x}$)-dependency of the dielectric constant ε_r, those empirical mixing models and mixing corrections require many experimental data and show large inaccuracies when the model extrapolates from the fitted data.

Models for the mixed solvent dielectric constant ε_r were specifically developed and applied in the context of e-EoS. Maribo-Mogensen et al. [9] predict the dielectric constant ε_r of associating mixtures by extending the framework of Onsager [23], Kirkwood [18], and Fröhlich [24]. For this purpose, the authors calculate the liquid volume and the probability of association using a cubic-plus-association EoS with a Wertheim association model [25–29]. From analyzing the molecular orientation and the hydrogen-bonding network, the developed model predicts the mixed solvent dielectric constant ε_r over a wide range of temperature and pressure. The model by Maribo-Mogensen et al. [9] is applied in the electrolyte Cubic plus Association equation of state [30]. Langenbach and Kohns [15] calculate the dielectric constant ε_r from an orientation distribution function derived from their co-oriented fluid functional equation for electrostatic interactions (COFFEE). As models for only the dielectric constant ε_r, these two models are rather involved and require a certain degree of expert knowledge, e.g., the analysis of molecular orientation [9], or the use of certain e-EoS [15].

In conclusion, a simple yet physical model is needed for the dielectric constant ε_r of pure solvents and solvent mixtures for the application within e-EoS. Already in 1983, Tani et al. [31] applied perturbation theory to derive an expression for the dielectric constant ε_r of a dipolar fluid. For a Stockmayer fluid, the authors compared their result to computational simulations for the dielectric constant ε_r and found perturbation theory to be a promising approach. In following work, Kalikmanov [32] applied the algebraic perturbation technique by Ruelle [33] and confirmed the result of Tani et al. [31] after correcting the calculation of the three-body terms according to Szalai et al. [34–36]. Recently, Kohns et al. [37] critically assessed the use of perturbation theories for the dielectric constant. The authors investigated Stockmayer fluids by comparing results from molecular simulation with perturbation theory models for low density. In agreement with Tani et al. [31], the authors highlight the potential of perturbation theories for modeling the dielectric constant ε_r.

This study presents a physical model for the dielectric constant ε_r of mixtures of real solvents based on perturbation theory. For this purpose, we modify the perturbation theory approach by Tani et al. [31] for real fluids and extend it to mixtures. Our model depends on temperature, density, and mixture composition. For each pure component, the model requires the dipole moment and one to two parameters fit to pure component data for the dielectric constant ε_r. We apply our model to water, methanol, ethylene glycol, and their mixtures considering pure component experimental data ranging from 273.15 K to 823.15 K and from 0.1 MPa to 1189.0 MPa. Even in the case of scarce experimental data for the pure component, the presented model accurately predicts the mixed solvent dielectric constant ε_r. The model offers promising predictive power for mixtures.

2. Perturbation theory and model for dielectric constant ε_r

In agreement with Tani et al. [31], Kalikmanov [36] applies perturbation theory to the dielectric constant ε_r, arriving at

$$\varepsilon_r - 1 = 3y\left[1 + y + \left(\frac{17}{16}I - 1\right)y^2\right] \tag{8}$$

where I is a three-body correlation integral and y is the dipole density

$$y \equiv \frac{4\pi}{9}\beta\rho\mu^2 \tag{9}$$

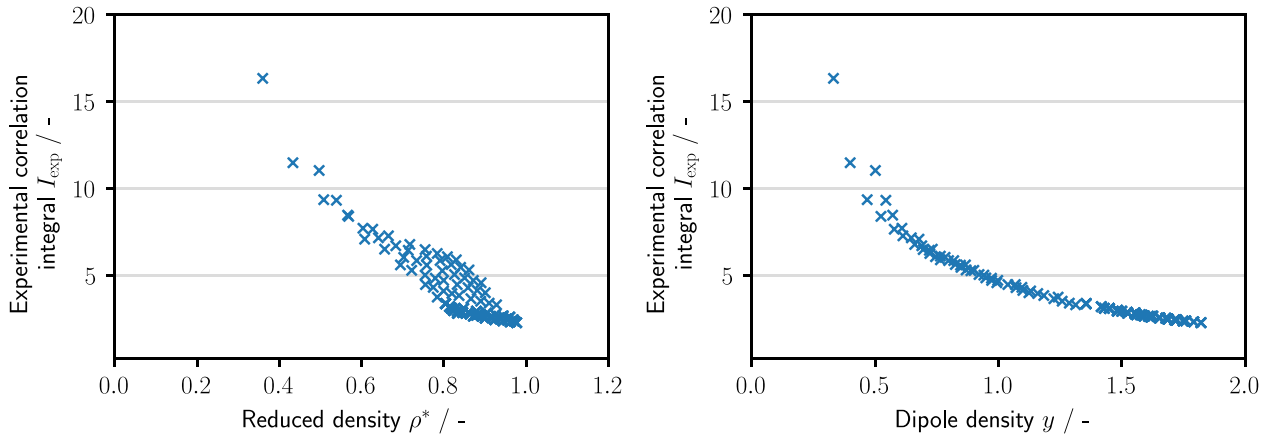

Fig. 1. Experimental data for correlation integral I_{exp} of methanol calculated with Equation (12) depending on the density ρ (a) and the dipole density y (b). Experimental data from Mohsen-Nia et al. [41], Srinivasan and Kay [42], Dannhauser and Bahe [43], and Heger [44] for temperatures between 283.15 K and 573.15 K and pressures between 0.1 MPa and 350 MPa.

with $\beta = 1/(k_B T)$ as the reciprocal of the thermodynamic temperature T, ρ as the density of molecules, and μ as the dipole moment of the molecule. Since the dipole density y is dimensionless, the units must be converted accordingly, e.g., ρ in $Å^{-3}$ and μ^2 in $J \cdot Å^3$. The correlation integral I in Kalikmanov's work [36] is related to the correlation integral $I_{dd\Delta}$ proposed by Tani et al. [31] by a factor, with

$$I = I_{dd\Delta} \frac{9}{17\pi^2\sigma^6}, \tag{10}$$

where σ is a size parameter. This factor ensures a convenient (dimensionless) low-density limit of $I(\rho = 0) = 1$. Equation (8) leads to the exact low-density limit Wertheim [38] also proposed for the mean spherical approximation (MSA). However, alternative expansions are possible. Rushbrooke [39] and Tani et al. [31] argue that the expansion according to Equation (8) is robust for extrapolation to high densities. In contrast, expansions in terms of the Debye term $(\varepsilon_r - 1)/(\varepsilon_r + 2)$ and in terms of the Kirkwood [18] term $(\varepsilon_r - 1)(2\varepsilon_r + 1)/(9\varepsilon_r)$ are less well-behaved for high densities [31,40]. In this work, we modify Equation (8) for the application to non-spherical, real fluids and extend the expression to mixtures.

2.1. Application to real, non-spherical fluids

Tani et al. [31] and Kalikmanov [36] apply their theory to a polar model fluid, i.e., a system of hard spheres with the diameter σ and point dipoles. To model real, non-spherical fluids, we account for the non-sphericality by scaling the dipole density y. For this purpose, we introduce the dipole density scaling parameter a_1 as a component-specific adjustable parameter of our model. The scaled dipole density y^* is then calculated as

$$y^* = a_1 \cdot y = a_1 \cdot \frac{4\pi}{9} \beta \rho \mu^2. \tag{11}$$

Initially, Tani et al. [31] introduce the correlation integral I as a function of the reduced density $\rho^* = \rho\sigma^3$. To get an impression of the correlation integral I, we solve Equation (8) for I and use experimental data for the (unscaled) dipole density y_{exp} and the dielectric constant $\varepsilon_{r,exp}$ to calculate the experimental correlation integral I_{exp}:

$$I_{exp}(y_{exp}) = \frac{16}{17}\left[1 + \frac{1}{y_{exp}^2} \cdot \left(\frac{\varepsilon_{r,exp} - 1}{3y_{exp}} - 1 - y_{exp}\right)\right] \tag{12}$$

Fig. 1 shows the obtained experimental correlation integral I_{exp} as a function of the reduced density ρ^* (left) and the dipole density y (right) for methanol. Generally, the correlation integral I decreases with increasing reduced density ρ^*. However, the experimental correlation integral I_{exp} is not a univariate function of density (but is a function of density and temperature). In contrast, a distinct, almost univariate relationship is observed between the experimental correlation integral I_{exp} and the dipole density y_{exp}. Consequently, an ansatz function for the correlation integral I depending on the dipole density y seems favorable.

Fig. 1 additionally shows that the experimental data for I_{exp} do no exhibit the theoretical low-density limit of $I(\rho \to 0) \to 1$, according to Wertheim [38], but diverge for low densities. However, in Equation (8), the influence of the correlation integral I on the result for the dielectric constant ε_r becomes negligible for low densities. Therefore, the ansatz function for the correlation integral I does not have to agree with the experimental data I_{exp} for low densities to achieve good results for the dielectric constant ε_r.

Overall, the ansatz function should fulfill the theoretical low-density limit of 1 and agree well with the experimental correlation integral I_{exp}. To account for the non-sphericality of real molecules, we define our ansatz function based on the scaled dipole density y^* (cf., Equation (11)). Based on the analysis of the experimental correlation integral and the theoretical low-density limit, we express our ansatz function as

$$I(y^*) = 1 + a_2 \cdot \left(e^{-y^*} - 1\right) \tag{13}$$

with the correlation integral parameter $a_2 \leq 1$ as the second component-specific adjustable parameter.

As an example, Fig. 2 shows the experimental correlation integral for methanol (blue dots) and our ansatz function for the correlation integral (green line) depending on the scaled dipole density y^* for a fixed dipole density scaling parameter a_1. Both dipole density scaling parameter a_1 and correlation integral parameter a_2 are fitted to experimental data for the dielectric constant ε_r (cf., Section 3). The ansatz function agrees well with the scaled experimental correlation integral at high densities and matches the theoretical low-density limit. At low densities, the dielectric constant ε_r is less sensitive to the correlation integral I than at high densities. As demonstrated in Fig. 2, the low-density limit shows divergence of the correlation integral $I(\varepsilon_r^{\pm 10\%})$ (red line) which denotes the correlation integral leading to an error of ±10% for the dielectric constant ε_r. All experimental data points within the red area correspond to an error of less than ±10%. Thus, the proposed ansatz function describes the experimental data well while obeying the theoretical low-density limit.

Note that Equation (8) produces an unphysical maximum of the dielectric constant ε_r at high densities if the pre-factor of $(y^*)^3$

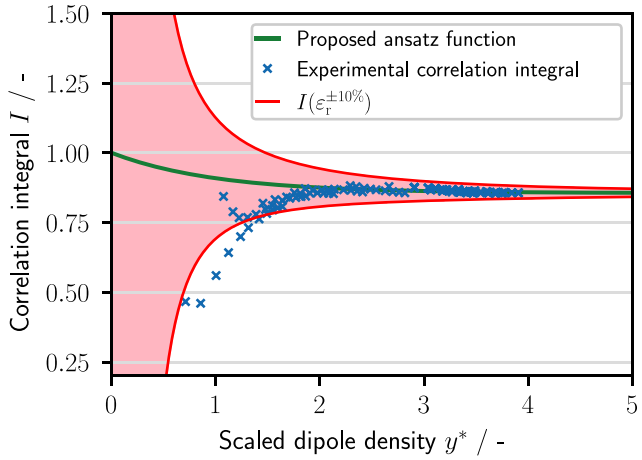

Fig. 2. Experimental data (blue) and proposed ansatz for the correlation integral (green) depending on scaled dipole density y^*. The chosen ansatz function must fulfill the low-density limit of 1. The dipole density scaling parameter a_1 is 2.145 and the correlation integral parameter a_2 is 0.1442 (cf., Section 3.2). The red lines correspond to a correlation integral $I(\varepsilon_r^{\pm 10\%})$ leading to a model error of maximal ±10% for methanol. (For interpretation of the references to colour in this figure legend, the reader is referred to the web version of this article.)

becomes negative. In the high-density limit, the proposed ansatz function $I(y^*)$ becomes $1 - a_2$. Thus, the pre-factor $((17/16)I - 1)$ of $(y^*)^3$ in Equation (8) is negative if a_2 is greater than $1/17$. However, the maximum of our ansatz function from Equation (13) occurs at densities that are either not physical themselves or not relevant in practice. We recommend including liquid-phase experimental data in the parameter fit to ensure physical behavior for densities relevant in practice.

An estimate for a limiting scaled dipole density y^* depending on the temperature and the parameters can be obtained by numerically solving for the maximum of the dielectric constant ε_r by setting the derivative to 0, as

$$\left.\frac{\partial \varepsilon_r}{\partial y^*}\right|_T = 3\cdot\left[1 + 6y^* + 3(y^*)^2 \cdot \left(\frac{17}{16}\left(1 + a_2 \cdot (e^{-y^*} - 1)\right) - 1\right) - \frac{17}{16} \cdot a_2 \cdot (y^*)^3 \cdot e^{-y^*}\right] \stackrel{!}{=} 0 \tag{14}$$

for $y^* > 0$. The limiting dipole density y^*_{max} can be converted to the limiting density ρ_{max} by

$$\rho_{max} = \frac{9 \cdot k_B T}{4\pi \cdot \mu^2 \cdot a_1} \cdot y^*_{max}. \tag{15}$$

The limiting densities ρ_{max} of the substances under study exceed the maximum experimental densities by at least 35 %, 90 %, and 165 % for water, methanol, and ethylene glycol, respectively. An alternative ansatz function that ensures a physical high-density limit for the dielectric constant ε_r is proposed in Section S3 of the Supporting Information. However, we observed that this alternative ansatz function leads to somewhat higher deviations of the model from experimental data and is thus not further considered in the following.

2.2. Extension to mixtures

To extend our model towards mixed solvent dielectric constants, mixing rules are introduced for the dipole density y^* and the correlation integral I. These mixing rules enable calculating mixed solvent dielectric constants based on pure component parameters and mixture densities $\rho(T, p, \mathbf{x})$. Thus, no experimental data for mixed solvents is required for parametrization.

The scaled dipole density y^* is expressed based on the partial dipole density. Thus, Equation (11) is extended to the mixture of n components by

$$y^* = \frac{4\pi}{9}\beta \sum_{i=1}^{n} a_{1,i} \cdot \rho_i \mu_i^2 \tag{16}$$

with the partial density $\rho_i = x_i \rho$, the dipole moment μ_i and the dipole density scaling parameter $a_{1,i}$ of component i. We express the correlation integral $I(y^*)$ based on the mole fraction x_i of component i, as

$$I(y^*) = 1 + \left(\sum_{i=1}^{n} a_{2,i} x_i\right) \cdot \left(e^{-y^*} - 1\right) \tag{17}$$

with the pure component correlation integral parameter $a_{2,i}$ and the scaled dipole density y^* of the mixture from Equation (16).

If experimental data is available for the mixed solvent dielectric constant ε_r, the scaled dipole density y^* (Equation (16)) can be refined by introducing a binary parameter ψ_{ij} of components i and j (cf., Section 4.3 below).

In conclusion, we model the dielectric constant ε_r of the mixed solvent as a univariate function of the dipole density y based on perturbation theory according to Tani et al. [31]. Apart from the dipole moment μ_i and a thermodynamic model for the mixture density $\rho(T, p, \mathbf{x})$, the model requires two parameters per component fitted to experimental data of pure components: the dipole density scaling parameter a_1 and the correlation integral parameter a_2. The proposed model is thus given through Equations (16), (17), and (8), where the scaled dipole density y^* is used instead of the dipole density y.

3. Correlation results for pure substances

For each pure component i, the dipole density scaling parameter $a_{1,i}$ and correlation integral parameter $a_{2,i}$ are fitted to experimental data for the dielectric constant ε_r. In this work, the fit is a least-squares minimization of the absolute deviation between the experimental and the calculated data with the total squared residuum $\delta\varepsilon_r$ for all m data points

$$\delta\varepsilon_r = \sum_{i=1}^{m}\left(\varepsilon_{r,model,i} - \varepsilon_{r,exp,i}\right)^2 \tag{18}$$

with the dielectric constant $\varepsilon_{r,model,i}$ of the proposed model and the experimental dielectric constant $\varepsilon_{r,exp,i}$ for data point i. The order of magnitude for the dielectric constant ε_r varies from 10^0 to 10^2. The technically most relevant dielectric constants are the high values for the dielectric constants in the liquid phase. Thus, we minimize the absolute deviation instead of the relative deviation. In contrast, minimizing the relative deviation would emphasize the result for low dielectric constants, i.e., in the gas phase, while larger absolute deviations would be observed in the liquid phase.

We adjust the pure component parameters for water, methanol, and ethylene glycol. The dipole density scaling parameter $a_{1,i}$ and the correlation integral parameter $a_{2,i}$ resulting from this fit are listed in Table 1 with their corresponding number of data points m, dipole moment μ_i and mean absolute relative deviation (MARD). The MARD between the model results $\varepsilon_{r,model,i}$ and the experimental data points $\varepsilon_{r,exp,i}$ for m data points is defined as

$$MARD = \frac{1}{m} \cdot \sum_{i=1}^{m}\left|\frac{\varepsilon_{r,model,i} - \varepsilon_{r,exp,i}}{\varepsilon_{r,exp,i}}\right|. \tag{19}$$

The quality of the parameter fit is analyzed using the MARD instead of the total squared residuum from Equation (18) because we consider MARD values as more intuitive measures for mean deviations from experimental data.

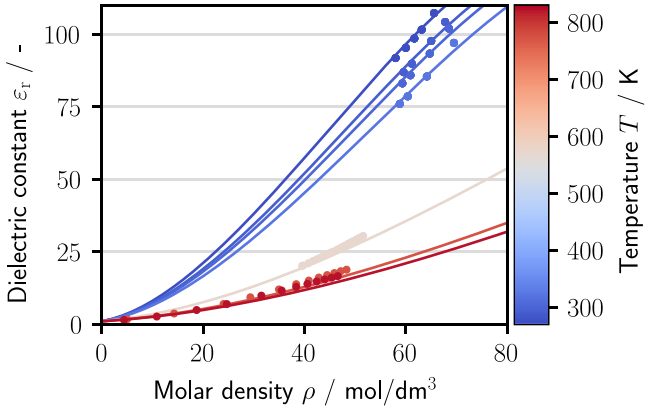

Fig. 3. Dielectric constant ε_r of pure water depending on molar density ρ and temperature T. The 149 experimental data points from Fernández et al. [46] (dots) range from 273.15 K to 823.15 K and from 8.6 MPa to 1190.0 MPa. The results of the proposed model are shown as solid lines.

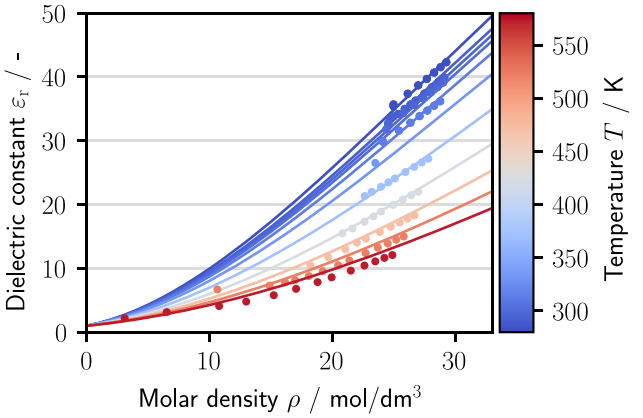

Fig. 4. Dielectric constant ε_r of pure methanol depending on molar density ρ and temperature T. The 163 experimental data points from Mohsen-Nia et al. [41], Srinivasan and Kay [42], Dannhauser and Bahe [43], and Heger [44] (dots) range from 283.15 K to 573.15 K and from 0.1 MPa to 350 MPa. The results of the proposed model are shown as solid lines.

If not provided in the literature with the experimental data, the molar densities are calculated using the REFPROP database [45]. If the model is used in the context of e-EoS, the densities can be calculated directly using the e-EoS.

3.1. Water

Fig. 3 illustrates the isotherms of the dielectric constant ε_r of water for varying molar density ρ in a temperature range of 273.15 K to 823.15 K. The model results in a mean average relative deviation of MARD = 3.2 % (cf., Table 2). For temperatures below 500 K, the model is more accurate (MARD= 1.2 %) than for higher temperatures (MARD= 7.5 %). If a specific application requires more accurate results for high temperatures, the fit could be improved by adapting the weighting for higher temperatures in the least-squares fit.

The model shows good agreement with the experimental data, confirming that deviations in the ansatz function, Equation (17), from experimentally deduced values for the correlation integral I_{exp} at low densities are indeed insensitive and do not cause trouble (cf., Section 2.1). Thus, the presented model captures a wide range of temperature and pressure, even supercritical states.

3.2. Methanol

For methanol, the experimental data used for the parameter fit cover a temperature range of 283.15 K to 573.15 K (Fig. 4). On average, the model deviates from the experimental data by MARD = 3.0 % (Table 1) and thus, a similar accuracy is obtained as for water: as desired, the model results are more accurate for technically relevant states, i.e., the liquid phase at lower temperatures and higher densities, than above or near the critical point. For temperatures below 500 K, an MARD of 1.5 % is obtained.

3.3. Ethylene glycol

Comprehensive experimental coverage of temperature-pressure (T, p)-states is available for a limited number of substances. For many species, only a limited number of experimental data is available. We are therefore interested in the model robustness for cases with scarce experimental data. For ethylene glycol, we thus mimic a situation where only a single experimental data point, at 303.15 K, is available. To prevent overfitting, we adjust only the dipole density scaling parameter $a_{1,i}$ to the data point at 303.15 K. In contrast, the correlation integral parameter $a_{2,i}$ is set equal to the correlation integral parameter of water. We fit the dipole density scaling parameter $a_{1,i}$ instead of the correlation integral parameter $a_{2,i}$, because the correlation integral parameter $a_{2,i}$ takes similar values for water and methanol and acts less strongly on ε_r compared to the dipole density scaling parameter $a_{1,i}$.

The available experimental data for ethylene glycol covers temperatures from 278.15 K to 423.15 K [47]. We use that data to assess the model's robustness for predicting wide temperature and pressure ranges not covered in the parameter regression. Furthermore, we assess the model's robustness for predicting mixed solvent dielectric constants for ethylene glycol-water (cf., Section 4.2).

The pure component dielectric constant ε_r of ethylene glycol is shown in Fig. 5 for a temperature range of 278.15 K to 423.15 K. With 0.6 %, the MARD of all data points not included in the parameter fit is small compared to water and methanol (Table 1). However, the studied states for ethylene glycol are far below the critical point, similar to the technically relevant states for water and methanol, which also exhibit more accurate model results.

A similar extrapolation capability of our model is obtained for water and methanol, which is analyzed by adjusting both model parameters to only two experimental data points at varying temperatures (for details, please see Supporting Information,

Table 1
Pure component parameters for water, methanol, and ethylene glycol: Dipole density scaling parameter $a_{1,i}$, correlation-integral parameter $a_{2,i}$, number of data points m, dipole moment μ_i and mean absolute relative deviation (MARD) of dielectric constant ε_r of the proposed model compared to experimental data. For ethylene glycol, the MARD is calculated compared to the 23 data points not included in the fit, because the MARD compared to the fit point is 0.

Fluid	Dipole density scaling parameter $\mathbf{a_{1,i}}$	Correlation integral parameter $\mathbf{a_{2,i}}$	# Data points m for fit	Dipole moment $\boldsymbol{\mu_i}$ in Debye	MARD (%)
Water	1.465	0.1215	149	1.855	3.2
Methanol	2.145	0.1442	163	1.700	3.0
Ethylene glycol	1.656	0.1215 ($= a_{2,water}$)	1	2.410	0.6

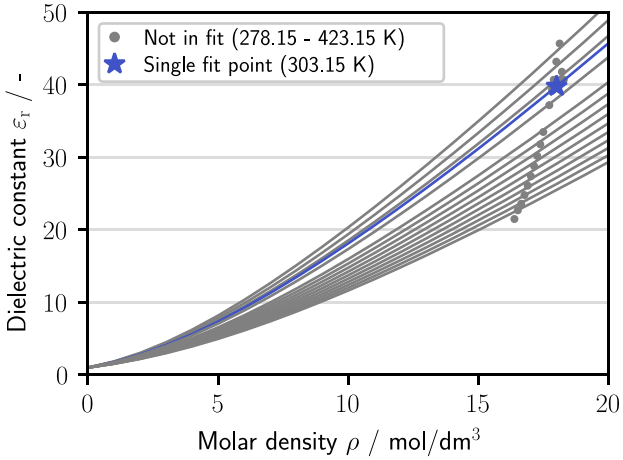

Fig. 5. Dielectric constant ε_r of pure ethylene glycol depending on molar density ρ and temperature T. The experimental data from the Dortmund Data Bank [47] (dots) range from 278.15 K to 423.15 K. The results of the proposed model are indicated as solid lines. The star marks the single point that was used for determining the dipole density scaling parameter a_1 (see text) and the solid blue line shows the model results for the temperature of the single fit point. Model results and experimental data points in grey are not included in the parameter fit, they are predictions of the model.

Section S1). By considering two low temperatures, the technically relevant liquid states can be accurately predicted (MARD of 1.2 % for water and 3.0 % for methanol). Including an experimental data point at a higher temperature refines the predictions also for higher temperatures (MARD of 5.1 % for water and 9.7 % for methanol). In conclusion, the model has strong extrapolation capabilities for the pure component dielectric constant ε_r, leading to accurate results even though the parameters are adjusted to only one or two data points.

We compare the proposed model for pure component dielectric constants ε_r to comparable models from the literature: an approach based on the model of Kirkwood [18] (cf., Equation (3)) and the model of Zhuang et al. [48] (details in the Supporting Information (cf., Section S2)). Both models have one adjustable parameter, and are thus characterized by lean parametrization and simple application. We adjust the model parameters to the full experimental data set for water and methanol used in our paper. Both one-parameter models from the literature achieve similar accuracies as our model if only a small temperature range is studied. However, due to the second adjustable parameter, our model achieves high accuracies for the dielectric constant ε_r in a wide range of temperatures and pressures.

4. Prediction of mixed solvent dielectric constants

Using the parameters obtained in the pure component parameter fit (cf., Section 3), we predict the mixed solvent dielectric constants ε_r for the mixtures methanol–water and ethylene glycol–water.

4.1. Mixture: Methanol–water

In Fig. 6, the mixed solvent dielectric constant ε_r is illustrated for various mole fractions of methanol x_{MeOH} and four temperatures in the range 293.15 K to 473.15 K. With 4.0 %, the MARD of the mixture predictions for methanol–water is 3.0 percentage points higher than for the pure component fits at similar temperatures (Table 2). The predictions for data points from Smith et al. [49] are less accurate than for the data points from Akerlöf [50] and Teutenberg et al. [51].

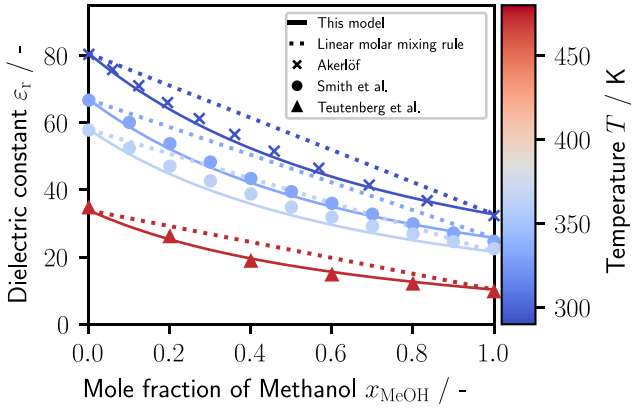

Fig. 6. Mixed solvent dielectric constant ε_r for methanol–water over mole fraction of methanol x_{MeOH}: experimental data from Akerlöf [50] (crosses), Smith et al. [49] (dots), and Teutenberg et al. [51] (triangles), model results from this work (solid lines), results of linear molar mixing rule (dashed line).

The results of the presented model are compared to the common linear mixing rules (Table 2), which mix the pure component dielectric constants $\varepsilon_{r,i}$ based on the composition Φ_i (cf., Equation (1)). In Equation (1), the composition Φ_i can be the mole fraction $\Phi_{\mathbf{x},i}$, the mass fraction $\Phi_{\mathbf{w},i}$, or the volume fraction $\Phi_{\mathbf{v},i}$.

The linear mixing rules require data for the pure component dielectric constants. Because the experimental data for the pure component dielectric constant is not available for each data series under study, we use the pure component dielectric constants $\varepsilon_{r,i}$ obtained from the presented model for the linear mixing rule.

The linear molar mixing rule leads to an MARD of 10.6 %, the linear mass-based mixing rule to an MARD of 2.5 %, and the linear volume-based mixing rule to an MARD of 3.6 %. Thus, the mass-based, the volume-based, and the presented model yield similar accuracies, while the MARD of the molar mixing rule is two to four times higher. The predictions using the linear molar mixing rule are particularly weak for the equimolar mixture (cf., Fig. 6).

4.2. Mixture: Ethylene glycol–water

The mixed solvent dielectric constant ε_r is analyzed for ethylene glycol–water depending on the mole fraction of ethylene glycol x_{EG} for eight temperatures in the range of 278.15 K to 373.15 K (Fig. 7). For ethylene glycol, only the dipole density scaling parameter $a_{1,i}$ is fitted to one data point, while the correlation integral parameter $a_{2,i}$ is set equal to the value of water (cf., Section 3.3).

With an MARD of 2.6 %, the prediction accuracy for the mixture ethylene glycol–water is in the same order of magnitude as for methanol–water. In particular, the model accurately extrapolates in temperature, highlighting the predictive power of the model.

Table 2
Number of data points for mixed solvent dielectric constant and mean absolute relative deviation for mixtures methanol–water and ethylene glycol–water: The mixed solvent dielectric constant ε_r is calculated using the model from this work vs. the linear mixing rules based on the mole fraction $\Phi_{\mathbf{x}}$, the mass fraction $\Phi_{\mathbf{w}}$, and the volume fraction $\Phi_{\mathbf{v}}$.

Mixture	# Data points	MARD (%)			
		This work	Linear mixing based on		
			$\Phi_{\mathbf{x}}$	$\Phi_{\mathbf{w}}$	$\Phi_{\mathbf{v}}$
Methanol–water	39	4.0	10.6	2.5	3.6
Ethylene glycol–water	80	2.6	8.6	4.0	3.0

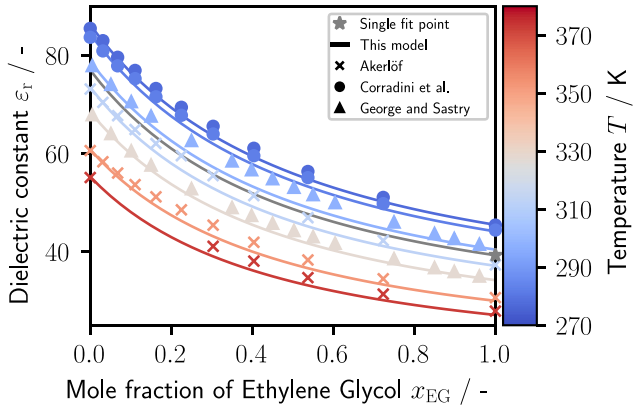

Fig. 7. Mixed solvent dielectric constant ε_r for ethylene glycol-water over the mole fraction of ethylene glycol x_{EG}. The experimental data stems from Akerlöf [50] (crosses), Corradini et al. [52] (dots), and George and Sastry [53] (triangles). The model results from this work are shown as solid lines. The grey star and the grey line show the single fit point and the model results at the temperature of single fit point, respectively.

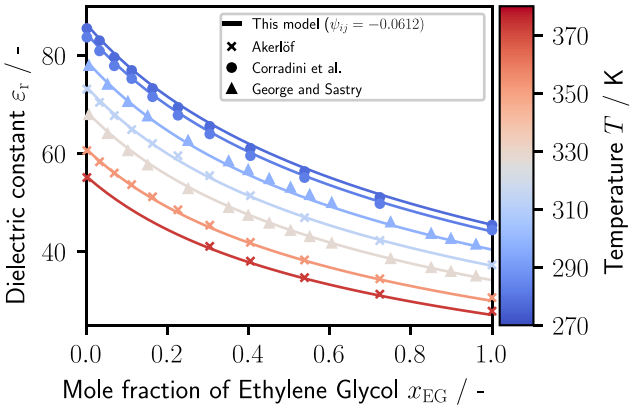

Fig. 8. Mixed solvent dielectric constant ε_r for ethylene glycol-water over the mole fraction of ethylene glycol x_{EG} with model from Equations (8) and (20). The experimental data stems from Akerlöf [50] (crosses), Corradini et al. [52] (dots), and George and Sastry [53] (triangles). The model results (solid lines) are calculated using a binary parameter of $\psi_{ij} = -0.0612$ to correct the scaled dipole density y^* (cf., Equation (20)).

Similarly to the mixture methanol–water, the accuracy of the predictions using the linear mass-based mixing rule (MARD of 4.0 %), linear volume-based mixing rule (MARD of 3.0 %), and the proposed model (MARD of 2.6 %) are similar, while the linear molar mixing rule yields less accurate results (MARD of 8.6 %). In contrast to methanol–water, the most accurate predictions are achieved by our model (Table 2). Overall, our model achieves a good accuracy for predicting mixed solvent dielectric constants even in the case of scarce data availability.

The analysis of the accuracy does not yield a clear preference for our model, the linear mass-based, and the linear volume-based mixing rule. In contrast, the linear molar mixing rule is least accurate. However, the linear mixing rules have conceptual deficiencies if the pure components are not stable in the same phase (at given temperature and pressure) as the regarded mixture (cf., Section 1). Additionally, the linear mixing rules need many experimental data or other models for the pure component dielectric constants $\varepsilon_{r,i}$, while our model provides a unified framework for determining dielectric constants ε_r of pure solvents and solvent mixtures. In particular, the lean parametrization and the extrapolation capability are promising for predictive contexts, e.g., solvent screenings or computer-aided molecular design.

4.3. Model refinement using a binary parameter

If experimental data for the mixed solvent dielectric constant ε_r is available, the proposed model from Equation (8) can be refined by introducing a binary parameter $\psi_{ij} = \psi_{ji}$ for the scaled dipole density y^* of a mixture of the components i and j. This binary parameter ψ_{ij} is fitted to the experimental data for the mixed solvent dielectric constant ε_r. The expression for the scaled dipole density y^* from Equation (16) is modified as

$$y^* = \frac{4\pi}{9}\beta\rho\sum_{i=1}^{n}\sum_{j=1}^{n}x_i x_j \frac{\mathrm{a}_{1,i}\mu_i^2 + \mathrm{a}_{1,j}\mu_j^2}{2}\cdot(1-\psi_{ij}) \tag{20}$$

with the reciprocal of the thermodynamic temperature β, the mixture density ρ, the mole fractions x_i and x_j, the dipole density scaling parameters $\mathrm{a}_{1,i}$ and $\mathrm{a}_{1,j}$, and the dipole moments μ_i and μ_j of components i and j, respectively. For $i = j$, the binary parameter ψ_{ij} is set to 0 to ensure consistent pure component dielectric constants $\varepsilon_{r,i}$. If the binary parameter ψ_{ij} is set to 0, Equation (20) reduces to the original definition of the scaled dipole density y^* from Equation (16).

For the mixture methanol–water, we fit the binary parameter ψ_{ij} to mixture data for the dielectric constant ε_r from Akerlöf [50], Smith et al. [49], and Teutenberg et al. [51]. We obtain an optimal binary parameter of $\psi_{ij} = -0.0635$ improving the MARD from 4.0 % to 2.9 %. The overall improvement of the model is rather low. However, it is noteworthy that the deviations to data from Akerlöf [50] and from Smith et al. [49] are substantially decreased, whereas the data from Teutenberg et al. [51] is not described well.

For the mixture ethylene glycol–water, we use mixture data for the dielectric constant ε_r from Akerlöf [50], Corradini et al. [52], and George and Sastry [53]. The resulting optimal binary parameter of $\psi_{ij} = -0.0612$ reduces the MARD from 2.6 % to 0.7 % (Fig. 8).

In conclusion, introducing a binary parameter ψ_{ij} adds an additional model parameter, but can significantly improve the model accuracy if experimental data is available for the mixed solvent dielectric constant ε_r: for the mixture methanol–water, the MARD is reduced by 28 % and for the mixture ethylene glycol–water by even more than 70 % compared to the purely predictive model for the mixture ($\psi_{ij} = 0$). However, experimental data for the mixed solvent dielectric constant ε_r is available only for a limited number of mixtures. If no experimental data is available for the mixed solvent dielectric constant ε_r, convincing results can be obtained using the proposed model without binary parameter ($\psi_{ij} = 0$) (cf., Sections 4.1 and 4.2).

5. Conclusion

This work presents a model for the dielectric constant ε_r of pure substances and solvent mixtures based on perturbation theory. For this purpose, we modify the model by Tani et al. [31] for real fluids and extend it to mixtures. As a result, we obtain a model which is third order in the dimensionless dipole density y. For each pure component, two parameters are fitted to experimental data of the dielectric constant ε_r: the dipole density scaling parameter $\mathrm{a}_{1,i}$ and the correlation integral parameter $\mathrm{a}_{2,i}$. For mixtures, mixing rules are proposed based on the partial dipole density (for $\mathrm{a}_{1,i}$) and on the mole fraction (for $\mathrm{a}_{2,i}$). Thus, the dielectric constant ε_r of mixed solvents can be predicted solely based on pure component parameters and the density of the mixture.

In the case of scarce experimental data availability, e.g., in the context of predictive electrolyte thermodynamics, we demonstrate for ethylene glycol that fitting only the dipole density scaling parameter $\mathrm{a}_{1,i}$ to one data point and taking the correlation integral parameter $\mathrm{a}_{2,i}$ of water can still lead to very good results.

The presented model has a sound physical basis, a lean parametrization and can easily be integrated into existing electrolyte equations of state. The model can be refined by introducing a binary parameter ψ_{ij} fit to mixture data if available.

We use the presented model to predict the mixed solvent dielectric constant ε_r for methanol–water and ethylene glycol–water. The model achieves accurate predictions for both mixtures under study: the mean absolute relative deviation is 4.0 % for methanol–water and 2.6 % for ethylene glycol–water. Furthermore, the prediction of the mixed solvent dielectric constant is largely improved compared to the linear molar mixing rule. Compared to the linear mass-based and volume-based mixing rules, comparable accuracies are observed. Even in the case of scarce experimental data availability, the presented model shows good extrapolation capability highlighting the high predictive power of our presented model. In the future, we plan to extend the model to account for the influence of ionic species on the dielectric constant.

Declaration of Competing Interest

None.

Acknowledgements

We appreciate helpful discussions with Philipp Rehner. Author J. Gross acknowledges funding by Deutsche Forschungsgemeinschaft (DFG, German Research Foundation) under Germany's Excellence Strategy - EXC 2075–390740016.

Supplementary material

Supplementary material associated with this article can be found, in the online version, at doi:10.1016/j.fluid.2021.113346.

References

[1] M.A. Makeev, N.N. Rajput, Computational screening of electrolyte materials: status quo and open problems, Curr. Opin. Chem. Eng. 23 (2019) 58–69, doi:10.1016/j.coche.2019.02.008.
[2] M. Moura de Salles Pupo, R. Kortlever, Electrolyte effects on the electrochemical reduction of CO_2, Chem. Phys. Chem. 20 (22) (2019) 2926–2935, doi:10.1002/cphc.201900680.
[3] M. Bülow, N. Gerek Ince, S. Hirohama, G. Sadowski, C. Held, Predicting vapor–Liquid equilibria for sour-Gas absorption in aqueous mixtures of chemical and physical solvents or ionic liquids with ePC-SAFT, Ind. Eng. Chem. Res. 60 (17) (2021) 6327–6336, doi:10.1021/acs.iecr.1c00176.
[4] G.M. Kontogeorgis, B. Maribo-Mogensen, K. Thomsen, The debye-Hückel theory and its importance in modeling electrolyte solutions, Fluid Phase Equilib. 462 (26) (2018) 130–152, doi:10.1016/j.fluid.2018.01.004.
[5] J.-P. Hansen, I.R. McDonald, Theory of simple liquids: With applications to soft matter, 4th ed., Academic Press, Amsterdam and Boston, 2013.
[6] D. Henderson, L. Blum, A. Tani, Equation of State of Ionic Fluids, in: K.-C. Chao (Ed.), Equations of state, ACS Symposium Series, 300, American Chemical Society, Washington, DC, 1986, pp. 281–296, doi:10.1021/bk-1986-0300.ch013.
[7] F. Drunsel, W. Zmpitas, J. Gross, A new perturbation theory for electrolyte solutions, J. Chem. Phys. 141 (5) (2014) 054103, doi:10.1063/1.4891360.
[8] L. Blum, D.Q. Wei, Analytical solution of the mean spherical approximation for an arbitrary mixture of ions in a dipolar solvent, J. Chem. Phys. 87 (1) (1987) 555–565, doi:10.1063/1.453604.
[9] B. Maribo-Mogensen, G.M. Kontogeorgis, K. Thomsen, Modeling of dielectric properties of complex fluids with an equation of state, J. Phys. Chem. B 117 (12) (2013) 3389–3397, doi:10.1021/jp310572q.
[10] C. Held, T. Reschke, S. Mohammad, A. Luza, G. Sadowski, ePC-SAFT revised, Chem. Eng. Res. Des. 92 (12) (2014) 2884–2897, doi:10.1016/j.cherd.2014.05.017.
[11] S. Prakongpan, T. Nagai, Solubility of acetaminophen in cosolvents, Chem. Pharm. Bull. (32) (1984) 340–343, doi:10.1248/cpb.32.340.
[12] M. Bülow, M. Ascani, C. Held, ePC-SAFT advanced - Part I: Physical meaning of including a concentration-dependent dielectric constant in the born term and in the Debye-Hückel theory, Fluid Phase Equilib. 535 (2021) 112967, doi:10.1016/j.fluid.2021.112967.
[13] M. Ascani, C. Held, Prediction of salting-out in liquid-liquid two-phase systems with ePC-SAFT: Effect of the Born term and of a concentration-dependent dielectric constant, Zeitschrift für anorganische und allgemeine Chemie 647 (12) (2021) 1305–1314, doi:10.1002/zaac.202100032.
[14] M. Kohns, Molecular simulation study of dielectric constants of pure fluids and mixtures, Fluid Phase Equilib. 506 (5) (2020) 112393, doi:10.1016/j.fluid.2019.112393.
[15] K. Langenbach, M. Kohns, Relative Permittivity of Dipolar Model Fluids from Molecular Simulation and from the Co-Oriented Fluid Functional Equation for Electrostatic Interactions, J. Chem. Eng. Data 65 (3) (2020) 980–986, doi:10.1021/acs.jced.9b00296.
[16] M. Bülow, X. Ji, C. Held, Incorporating a concentration-dependent dielectric constant into ePC-SAFT. An application to binary mixtures containing ionic liquids, Fluid Phase Equilib. 492 (2019) 26–33, doi:10.1016/j.fluid.2019.03.010.
[17] A. Zuber, L. Cardozo-Filho, V.F. Cabral, R.F. Checoni, M. Castier, An empirical equation for the dielectric constant in aqueous and nonaqueous electrolyte mixtures, Fluid Phase Equilib. 376 (9) (2014) 116–123, doi:10.1016/j.fluid.2014.05.037.
[18] J.G. Kirkwood, The dielectric polarization of polar liquids, J. Chem. Phys. 7 (10) (1939) 911–919, doi:10.1063/1.1750343.
[19] A.H. Harvey, J.M. Prausnitz, Dielectric constants of fluid mixtures over a wide range of temperature and density, J. Solution. Chem. (16 (10)) (1987), doi:10.1007/BF00650755.
[20] P. Wang, A. Anderko, Computation of dielectric constants of solvent mixtures and electrolyte solutions, Fluid Phase Equilib. 186 (1–2) (2001) 103–122, doi:10.1016/S0378-3812(01)00507-6.
[21] A.K. Amirjahed, M.I. Blake, Deviation of dielectric constant from ideality for certain binary solvent systems, J. Pharm. Sci. 64 (9) (1975) 1569–1570, doi:10.1002/jps.2600640936.
[22] A. Jouyban, S. Soltanpour, H.-K. Chan, A simple relationship between dielectric constant of mixed solvents with solvent composition and temperature, Int. J. Pharm. 269 (2) (2004) 353–360, doi:10.1016/j.ijpharm.2003.09.010.
[23] L. Onsager, Electric moments of molecules in liquids, J. Am. Chem. Soc. 58 (8) (1936) 1486–1493, doi:10.1021/ja01299a050.
[24] H. Fröhlich, Theory of dielectrics: Dielectric constant and dielectric loss, Monographs on the physics and chemistry of materials, 42, 2. ed., reprint, Clarendon Press, Oxford, 1990.
[25] M.S. Wertheim, Fluids with highly directional attractive forces. II. thermodynamic perturbation theory and integral equations, J. Stat. Phys. 35 (1–2) (1984) 35–47, doi:10.1007/BF01017363.
[26] M.S. Wertheim, Fluids with highly directional attractive forces. I. statistical thermodynamics, J. Stat. Phys. 35 (1–2) (1984) 19–34, doi:10.1007/BF01017362.
[27] M.S. Wertheim, Fluids with highly directional attractive forces. III. multiple attraction sites, J. Stat. Phys. 42 (3–4) (1986) 459–476, doi:10.1007/BF01127721.
[28] M.S. Wertheim, Fluids with highly directional attractive forces. IV. equilibrium polymerization, J. Stat. Phys 42 (3–4) (1986) 477–492, doi:10.1007/BF01127722.
[29] W.G. Chapman, G. Jackson, K.E. Gubbins, Phase equilibria of associating fluids, Mol. Phys. 65 (5) (1988) 1057–1079, doi:10.1080/00268978800101601.
[30] A. Schlaikjer, K. Thomsen, G.M. Kontogeorgis, eCPA: An ion-specific approach to parametrization, Fluid Phase Equilib. 470 (2018) 176–187, doi:10.1016/j.fluid.2017.12.008.
[31] A. Tani, D. Henderson, J.A. Barker, C.E. Hecht, Application of perturbation theory to the calculation of the dielectric constant of a dipolar hard sphere fluid, Mol. Phys. 48 (4) (1983) 863–869, doi:10.1080/00268978300100621.
[32] V.I. Kalikmanov, Algebraic perturbation theory for polar fluids: A model for the dielectric constant, Phys. Rev. E (59 (4)) (1999) 4085–4090, doi:10.1103/PhysRevE.59.4085.
[33] D. Ruelle, Statistical mechanics: Rigorous results, reprint, World Scientific, Singapore, 2007.
[34] Szalai, Chan, Henderson, Comment on "Algebraic perturbation theory for polar fluids: A model for the dielectric constant", Phys. Rev. E 62 (6 Pt B) (2000) 8846–8850, doi:10.1103/PhysRevE.62.8846.
[35] V.I. Kalikmanov, Reply to "Comment on 'Algebraic perturbation theory for polar fluids: A model for the dielectric constant'", Phys. Rev. E 62 (6) (2000) 8851–8853, doi:10.1103/PhysRevE.62.8851.
[36] V.I. Kalikmanov, Statistical physics of fluids, Springer Berlin Heidelberg, Berlin, Heidelberg, 2001, doi:10.1007/978-3-662-04536-7.
[37] M. Kohns, J. Marx, K. Langenbach, Critical assessment of perturbation theories for the relative permittivity of dipolar model fluids, Chem. Eng. Sci. 245 (2021) 116875, doi:10.1016/j.ces.2021.116875.
[38] M.S. Wertheim, Exact solution of the mean spherical model for fluids of hard spheres with permanent electric dipole moments, J. Chem. Phys. 55 (9) (1971) 4291–4298, doi:10.1063/1.1676751.
[39] G.S. Rushbrooke, On the dielectric constant of dipolar hard spheres, Mol. Phys. 37 (3) (1979) 761–778, doi:10.1080/00268977900103181.
[40] G.S. Rushbrooke, G. Stell, J.S. Høye, Theory of polar liquids, Mol. Phys. 26 (5) (1973) 1199–1215, doi:10.1080/00268977300102411.
[41] M. Mohsen-Nia, H. Amiri, B. Jazi, Dielectric constants of water, methanol, ethanol, butanol and acetone: measurement and computational study, J. Solut. Chem. 39 (5) (2010) 701–708, doi:10.1007/s10953-010-9538-5.
[42] K.R. Srinivasan, R.L. Kay, Structural considerations from dielectric measurements on the aliphatic alcohols, J. Solut. Chem. 4 (4) (1975) 299–310, doi:10.1007/BF00650388.
[43] W. Dannhauser, L.W. Bahe, Dielectric constant of hydrogen bonded liquids. III. superheated alcohols, J. Chem. Phys. 40 (10) (1964) 3058–3066, doi:10.1063/1.1724948.

[44] K. Heger, Thesis, Institut für Physikalische Chemie, Karlsruhe, 1969 Ph.D. thesis.
[45] M. Huber, A. Harvey, E. Lemmon, G. Hardin, I. Bell, M. McLinden, NIST Reference Fluid Thermodynamic and Transport Properties Database (REFPROP) Version 10 - SRD 23, 2018, (2018). doi:10.18434/T4/1502528.
[46] D.P. Fernández, A.R.H. Goodwin, E.W. Lemmon, J.M.H. Levelt Sengers, R.C. Williams, A formulation for the static permittivity of water and steam at temperatures from 238 k to 873 k at pressures up to 1200 MPa, including derivatives and debye–Hückel coefficients, J. Phys. Chem. Ref. Data 26 (4) (1997) 1125–1166, doi:10.1063/1.555997.
[47] Dortmund Data Bank, (2021).
[48] B. Zhuang, G. Ramanauskaite, Z.Y. Koa, Z.-G. Wang, Like dissolves like: a first-principles theory for predicting liquid miscibility and mixture dielectric constant, Sci Adv 7 (7) (2021), doi:10.1126/sciadv.abe7275.
[49] R. Smith, S. Lee, H. Komori, K. Arai, Relative permittivity and dielectric relaxation in aqueous alcohol solutions, Fluid Phase Equilib. 144 (1–2) (1998) 315–322, doi:10.1016/S0378-3812(97)00275-6.
[50] G. Akerlof, Dielectric constants of some organic solvent-water mixtures at various temperatures, J. Am. Chem. Soc. 54 (11) (1932) 4125–4139, doi:10.1021/ja01350a001.
[51] T. Teutenberg, S. Wiese, P. Wagner, J. Gmehling, High-temperature liquid chromatography. part III: determination of the static permittivities of pure solvents and binary solvent mixtures–implications for liquid chromatographic separations, J. Chromatogr. A 1216 (48) (2009) 8480–8487, doi:10.1016/j.chroma.2009.09.076.
[52] F. Corradini, L. Marcheselli, A. Marchetti, M. Tagliazucchi, L. Tassi, G. Tosi, A Non-Linear Correlation Model for the Relative Permittivity of Ternary Amphiprotic (Solvent) Mixtures, Aust. J. Chem. 46 (10) (1993) 1545, doi:10.1071/CH9931545.
[53] J. George, N. Sastry, Partial excess molar volumes, partial excess isentropic compressibilities and relative permittivities of water + ethane-1,2-diol derivative and water + 1,2-dimethoxyethane at different temperatures, Fluid Phase Equilib. 216 (2) (2004) 307–321, doi:10.1016/j.fluid.2003.11.013.